Diabetes Renders Photoreceptors Susceptible to Retinal Ischemia-Reperfusion Injury

David A. Antonetti,[1,2] Cheng-Mao Lin,[1] Sumathi Shanmugam,[1] Heather Hager,[1] Manjing Cao,[1,3] Xuwen Liu,[1] Alyssa Dreffs,[1] Adam Habash,[1] and Steven F. Abcouwer[1]

[1]Department of Ophthalmology and Visual Sciences, University of Michigan, Michigan Medicine, Kellogg Eye Center, Ann Arbor, Michigan, United States
[2]Department of Molecular and Integrative Physiology, University of Michigan, Ann Arbor, Michigan, United States
[3]Department of Ophthalmology, Shanghai General Hospital (Shanghai First People's Hospital), Shanghai Jiao Tong University School of Medicine, Shanghai, China

Correspondence: Steven F. Abcouwer, University of Michigan Medicine, Department of Ophthalmology and Visual Sciences, Kellogg Eye Center, 1000 Wall Street, Ann Arbor, MI 48105, USA; sabcouwe@umich.edu.

Received: August 23, 2024
Accepted: November 3, 2024
Published: November 21, 2024

Citation: Antonetti DA, Lin CM, Shanmugam S, et al. Diabetes renders photoreceptors susceptible to retinal ischemia-reperfusion injury. *Invest Ophthalmol Vis Sci.* 2024;65(13):46. https://doi.org/10.1167/iovs.65.13.46

Purpose. Studies have suggested that photoreceptors (PR) are altered by diabetes, contributing to diabetic retinopathy (DR) pathology. Here, we explored the effect of diabetes on retinal ischemic injury.

Methods. Retinal ischemia-reperfusion (IR) injury was caused by elevation of intraocular pressure in 10-week-old BKS db/db type 2 diabetes mellitus (T2DM) mice or C57BL/6J mice at 4 or 12 weeks after streptozotocin (STZ)-induced type 1 diabetes mellitus (T1DM), and respective nondiabetic controls. Retinal neurodegeneration was evaluated by retinal layer thinning, TUNEL staining, and neuron loss. Vascular permeability was evaluated as retinal accumulation of circulating fluorescent albumin. The effects of pretreatment with a sodium-glucose co-transporter (SGLT1/2) inhibitor, phlorizin, were examined.

Results. Nondiabetic control mice exhibited no significant outer retinal layer thinning or PR loss after IR injury. In contrast, db/db mice exhibited significant outer retina thinning (49%, $P < 0.0001$), loss of PR nuclei (45%, $P < 0.05$) and inner segment (IS) length decline (45%, $P < 0.0001$). STZ-induced diabetic mice at 4 weeks showed progressive thinning of the outer retina (55%, by 14 days, $P < 0.0001$) and 4.3-fold greater number of TUNEL$^+$ cells in the outer nuclear layer (ONL) than injured retinas of control mice ($P < 0.0001$). After 12 weeks of diabetes, the retinas exhibited similar outer layer thinning and PR loss after IR. Diabetes also delayed restoration of the blood-retinal barrier after IR injury. Phlorizin reduced outer retinal layer thinning from 49% to 3% ($P < 0.0001$).

Conclusions. Diabetes caused PR to become highly susceptible to IR injury. The ability of phlorizin pretreatment to block outer retinal thinning after IR suggests that the effects of diabetes on PR are readily reversible.

Keywords: diabetic retinopathy (DR), retinal ischemia, photoreceptors, ischemia reperfusion (IR), retinal degeneration

Diabetic retinopathy (DR) is clinically characterized by observable retinal vascular pathologies, including regions of ischemia, hemorrhages, microaneurysms, venous beading, permeability leading to diabetic macular edema (DME), and ultimately neovascularization resulting in proliferative DR (PDR).[1] Laser photocoagulation targeting regions of vasculature permeability and neovascularization, as well as pan-laser photocoagulation (PLP) are effective methods to control disease progression. In addition, cytokine neutralizing therapies targeting vascular endothelial growth factor A (VEGF-A) alone or both VEGF-A and angiopoietin 2 (Ang2) are effective treatment options for nonproliferative diabetic retinopathy (NPDR), PDR, and DME.[2,3] However, only approximately half of the patients with DME receiving these cytokine neutralizing therapies show significant benefit, and DR remains a leading cause of visual loss and blindness. New approaches and mechanistic understanding of the disease process is needed.

In addition to the well-described vascular alterations, diabetes also causes retinal neurodegeneration, known as diabetic retinal neuropathy (DRN), which has been observed in patients without overt vascular pathology and mainly affects the inner retina.[4] DRN is mainly associated with alterations in visual functions associated with the inner retina and with thinning of the retinal ganglion cell complex (GCC), which includes the retinal nerve fiber layer (RNFL), ganglion cell layer (GCL), inner plexiform layer (IPL), or the combined ganglion cell-inner plexiform layer (GC-IPL).[5] DRN is well modeled in diabetic mouse and rat models, where it is associated with inner retinal layer thinning, as well as the death and loss of retinal ganglion cells (RGC) and displaced amacrine cells (dAC) in the GCL.[6] Although DRN in patients with diabetes occurs prior to clinically observable vascular pathologies, research has not resolved whether DRN causes loss of vision, precedes all vascular abnormalities, are a consequence of occult vascular changes, or simply repre-

Investigative Ophthalmology & Visual Science

sent a separate pathology from DR. Comparison of rodent diabetic models revealed that inner retinal thinning failed to account for loss of visual acuity.[7] Recently, research showed that genetically targeting vascular endothelial cells with a mutant form of occludin that is resistant to VEGF-induced permeability prevented loss of visual acuity in mice, whereas inner retinal thinning was still observed.[8] Thus, the contribution of DRN to loss of vision in patients with diabetes needs to be clarified.

Research has also implicated a role for photoreceptors (PRs) in the etiology DR (reviewed in Refs. 6, 9, and 10). In fact, it has been suggested that dysfunction of PR and the retinal pigment epithelium (RPE), which supports them, may play a key role in the initiation of DR.[10,11] This diabetic PR dysfunction has been attributed to mechanisms such as oxidative stress, inflammation, abnormal ion fluxes, and diminished insulin receptor signaling.[10] Evidence for a causal role of PR in DR onset and progression includes a survey of patients with retinitis pigmentosa that found a reduced incidence of DR.[11–13] Studies in mice found that ablation of PR and inhibition of rod-specific phototransduction by gene deletion of rod transducin alpha subunit ($Gnat^{-/-}$ mice) blocked some of the effects of diabetes on the retina, including harmful superoxide production, capillary drop out, vascular leakage in the IPL and upregulation of several inflammatory genes.[14,15] However, superoxide production and vascular permeability in other retinal layers still increased in the diabetic $Gnat^{-/-}$ mice. In addition, pharmacological inhibition of the visual cycle prevented DR pathology in mice.[16] The visual cycle includes the chemical process for replenishment of 11-cis-retinal from all-trans-retinol by the RPE, which is required for sustained light-stimulated rhodopsin signal transduction in rod PR. In diabetic mice, inhibition of cis-retinal recycling with retinylamine (Ret-NH2) diminished retinal capillary degeneration, vascular albumin leakage, retinal superoxide production, and expression of inflammatory factors.[16] Thus, a lack of PR or diminished phototransduction in PR can prevent the onset or progression of experimental DR pathologies. This suggests that PR are somehow detrimentally altered by diabetes in a way that contributes to DR risk or progression.

Interestingly, studies in both humans and animals failed to identify consistent global morphological changes to the outer retina during diabetes. A recent review by Tonade and Kern[10] highlighted numerous animal and human studies examining ultrastructural changes in the outer retina observed with diabetes. Most of the studies failed to detect outer retinal ultrastructural changes in diabetes. Further, when changes were observed they were not consistent between studies, although one of the few consistent observations was S-cone loss. In contrast, studies in patients suggest that when diabetes is combined with ischemia, PR changes can be detected. In patients, diabetes causes retinal capillary loss and nonperfusion, collectively known as diabetic macular ischemia (DMI).[17] Studies comparing PR density and light sensitivity of ischemic regions to normally perfused retinal regions in patients with DMI have found that areas of capillary nonperfusion exhibit outer retina layer thinning, PR disorganization, diminished PR density, and decreased light sensitivity.[18–22] In addition, diabetes can cause loss of vessel density and lack of perfusion in the choroidal vasculature, collectively referred to as diabetic choroidopathy.[23] Choroidal vascular changes start prior to the onset of DR, can predict onset and progression of DR, and increase with severity of DR.[24–32] Importantly, recent studies have found that diminished choroidal vessel density and perfusion are also associated with impaired cone PR sensitivity and PR structural abnormalities, as indicated by altered ellipsoid zone reflectivity in optical coherence tomography (OCT) images.[23,33–35] These studies suggest that in the presence of diabetes PR become susceptible to ischemic injury; however, it should be noted that the normal retinas that served as comparators did not have ischemic regions to serve as proper controls.

Rodent intraocular pressure (IOP)-induced retinal ischemia reperfusion (IR) injury models are convenient means to study neurodegeneration and neuroprotective mechanisms.[36] The model recapitulates inner retinal neural changes observed in DR. In the mouse IOP IR model, inner retinal neurons, including RGC and dAC in the GCL, exhibit high mortality, and the inner layers exhibit progressive thinning after IR injury (for example see Ref. 37). In contrast, the vast majority of PR are spared after IR injury, with very little reduction in ONL thickness. This is surprising given that in this model both retinal and choroidal blood circulations are halted, such that the entire retina is ischemic. The reason for PR resistance to ischemia is not understood.[36] We previously demonstrated that the mouse IOP IR model also recapitulates additional aspects of DR pathology, including a dramatic and sustained alteration of the inner blood retinal barrier (iBRB), with increased vascular permeability associated with tight junction protein loss from the endothelial cell border.[37] This change in vascular permeability could be prevented in rats by anti-VEGF treatment[38,39] and in mice with faricimab treatment targeting both VEGF and Ang2,[40] revealing that mouse IOP-induced IR injury effectively models the vascular permeability alterations observed in DR, as interventions in the model are predictive of human therapeutic response.

Here, we describe a new model to explore the effects of diabetes on PR. Whereas IR injury induces an inner retinal thinning with minimal changes to the outer retina, and diabetes alone reveals no observable changes to the ultrastructure of the outer retina, IR applied to both type 1 and type 2 diabetic animals induced a profound synergistic effect, with outer retinal loss of approximately 50% due to increased apoptosis of PR over a 7-day time course. Importantly, short-term treatment with sodium-glucose cotransporter 1 and 2 (SGLT1/2) inhibitor, phlorizin, effectively prevented the outer retinal degeneration. These studies suggest that diabetes dramatically increases PR susceptibility to the IR injury and that the diabetes-IR model may provide insight into the effects of diabetes on PR physiology.

Methods

Animals

All mice were purchased from the Jackson Laboratory (Bar Harbor, ME, USA) and treated in accordance with the ARVO Statement for the Use of Animals in Ophthalmic and Visual Research and the guidelines established by the University of Michigan Institutional Animal Care and Use Committee (IACUC). For the type 2 diabetes model, homozygous male BKS.Cg-*Dock7*^{m}+/+*Lepr* ^{db}/J mice (Jackson Laboratories Strain #:000697, referred to as db/db) were used, with heterozygous littermates (db/+) used as nondiabetic controls. For the type 1 diabetes, male C57BL/6J mice at 9 to 10 weeks of age were injected intraperitoneally with streptozotocin (STZ; 65 mg/kg body weight) for 5 consecutive days.

C57BL/6J mice injected with citrate buffer (pH 5.5) carrier alone were used as nondiabetic controls. Body weight and blood glucose levels of each mouse were monitored to track the progression of the disease. Blood glucose levels were determined with a test strip glucometer (Accu-Chek Nano; Roche) in the afternoon to avoid blood sugar spikes from overnight eating. STZ-treated mice that displayed glucose levels under 250 mg/dL were excluded from the study.

The IOP-induced retinal IR injury model was performed as previously described,[37] with elevation of IOP for 90 minutes via injection of saline into the anterior chamber of experimental IR eyes and needle puncture alone for contralateral sham control eyes. The IR procedure was performed on diabetic and control mice at 4 weeks or 12 weeks after STZ or citrate buffer treatment, or at 10 weeks of age for db/db and db/+ mice (which corresponds to 2–6 weeks of hyperglycemia). During ischemia, IOPs were consistently elevated to 85 to 95 millimeters of mercury (mm Hg); with mice rejected from the study if the IOP fell below 75 mm Hg during ischemia. Sham-treated eyes exhibited IOPs of 7 to 9 mm Hg, which is lower than normal IOP (13–15 mm Hg) due to heavy sedation. We did not observe any significant differences in IOPs of C57BL6/J, db/+ or db/db mice. In some experiments, the mice were treated with 400 mg/kg SGLT1/2 inhibitor phlorizin (a.k.a. phloridzin; Sigma, St. Louis, MO, USA) in 10% ethanol, 15% dimethyl sulfoxide, and 75% normal saline (0.9% w/v NaCl) by intraperitoneal injection at 16 and 1.5 hours before IOP elevation. Controls received injections of carrier alone. Blood glucose levels were measured with a drop of blood (approximately 2 µL) obtained from the tail vein using a glucometer.

Retinal Vascular Permeability Assay

Retinal vascular permeability was assessed by accumulation of fluorescein isothiocyanate-labeled bovine serum albumin (FITC-BSA; Sigma, St. Louis, MO, USA), as previously described.[39] To visualize regions of vascular leakage, the extravascular accumulation of sulfo-NHS-biotin was imaged as described previously.[41] Briefly, EZ-link Sulfo-NHS-biotin (300 mg/kg body weight, Thermo Fisher Scientific, Waltham, MA, USA) was perfused into the femoral vein of anesthetized mice and allowed to circulate for 5 minutes before transcardiac perfusion with warm saline for 2 minutes to flush vessels and then with 2% paraformaldehyde (PFA) for 3 minutes to fix the sulfo-NHS-biotin in place. Eyes were harvested and post-fixed in 1% PFA in PBS for 6 hours at 4°C prior to retinal dissection. Dissected retinas were probed with antibodies to endothelial marker CD31/PECAM1 (1:75, clone MEC 13-3, BD Bioscience #553370, San Jose, CA, USA), the tight junction protein ZO-1 (1:75, MABT11; Millipore Sigma, Burlington, MA, USA), and Texas Red Streptavidin (1:500, Vector Lab # SA-5006, Newark, CA, USA) by confocal microscopy. Quantification of sulfo-NHS-LC-biotin pixel intensity normalized by the area of the retinas was performed using ImageJ 1.54f software (Imagej.net).

In Situ Measurement of Retinal Layer Thicknesses

Retinal thickness was measured in situ in mice while they were under anesthesia using a small animal spectral domain optical coherence tomography (SD-OCT) imaging system (Envisu R2200; Bioptigen, Morrisville, NC, USA) and InVivoVue Diver software (Bioptigen). Measurements were made at 4 compass points 350 µm from the center of the optic nerve head and averaged. The total retina thickness was defined as the distance from the inner limiting membrane (ILM) to the RPE. The inner retina thickness was defined as the ILM to the inner limit of the outer plexiform layer (OPL) and the outer retina thickness was defined as the inner limit of the OPL to the RPE.

Cell Death Assay

Cell death was measured by detecting cytoplasmic histone associated DNA fragments using a Cell Death Detection ELISA kit (Cell Death Detection Assay; Roche Applied Science, Indianapolis, IN, USA) as described[38] and colorimetric signal was measured using a microplate spectrophotometer (FluoStar Omega, BMG Labtech, Ortenberg, Germany) to detect light absorbance at 405 nm with a 490 nm reference wavelength and normalized to total retina wet weight.

Terminal deoxynucleotidyl transferase dUTP nick end labeling (TUNEL) assays were performed in whole retinal flatmounts and retinal frozen sections using the Click-iT Plus TUNEL assay kit (Thermo Fisher Scientific). TUNEL in whole retinas was performed as previously described.[37] After the Click-iT reaction occurred, retinas were incubated with isolectin B4-AF488 (IB4, Molecular Probe I21411, Eugene, OR, USA; 1:75) and rabbit anti-Iba-1 (Wako 019-19741,1:200) in blocking buffer at 4°C overnight. After 5 to 6 washes with PBS plus 0.1% Tween 20 (PBST) for 1 hour each, the retinas were incubated with a mixture of secondary antibodies and Hoechst-33342 at 4°C overnight. After 5 to 6 washes with PBST for 1 hour each, the retinas were flat mounted in mounting media (Prolong Gold; Thermo Fisher Scientific). Immunofluorescence microscopy was performed using a Leica TSC SP5 confocal microscope. For TUNEL in retinal sections, immediately following euthanasia, the eyes were removed and fixed in 4% PFA in PBS for 1.5 hour at room temperature, then sequentially incubated in a gradient concentration of sucrose in PBS for cryoprotection (5% at room temperature for 1 hour, 10% at room temperature for 1 hour, and 20% at 4°C overnight). The eyes were then embedded with a 1:1 mixture of 20% sucrose and optimal cutting temperature compound (Tissue-Tek 4583; Sakura Finetek, Torrance, CA, USA) and cut into 30-µm thick sections. Retinal sections were permeabilized with 0.3% Triton X-100 in tris-buffered saline, placed in terminal deoxynucleotide transferase (TdT) reaction buffer from the Click-iT Plus TUNEL assay kit, and allowed to equilibrate for 20 minutes at 37°C. The TdT reaction buffer was replaced with a complete TdT reaction mixture and sections incubated for 75 minutes at 37°C to allow complete enzyme penetration into the tissue. Tissue sections were then rinsed 3 times 0.3% BSA in PBS and incubated in Click-iT TUNEL reaction cocktail for 60 minutes at 37°C to allow the Click-iT reaction to occur. The sections were again rinsed 3 times with 0.3% BSA in PBS, stained with Hoechst in 10% donkey serum, washed 2 times in Tris-buffered saline-Tween 20 (TBST), and then mounted and imaged with a DM6000 fluorescent microscope (Leica Microsystems, Inc., Buffalo Grove, IL, USA).

Retinal Layer Thickness Evaluation in Plastic-Embedded Sections

Eyes were branded to mark orientation and then enucleated. Enucleated eyes were fixed in 2% PFA and 2% glutaraldehyde overnight at 4°C, rinsed in PBS, and then dehydrated

Investigative Ophthalmology & Visual Science

in increasing ethanol concentrations (50%, 70%, 80%, 95%, and 100%) at room temperature for 30 minutes per step. The eyes were then embedded in JB-4 plastic using reagents from Electron Microscopy Sciences. The dehydrated eyes were first incubated in JB-4 Solution A (Cat# 14270-01) containing 1.25% catalyst (plasticized benzoyl peroxide, Cat# 14270-06) at 4°C overnight. The eyes were then embedded in a 25:1 mixture of Solution-A plus catalyst and JB-4 Solution B (Cat# 14270-04). Three-micron thin sections were stained for 30 to 60 seconds in Lee's Methylene Blue-Basic Fuchsin Stain containing 0.026% methylene blue, 0.026% basic fuchsin, 24% ethanol in 0.2M phosphate buffer, and pH 7.2, rinsed with water, 0.5% acetic acid, and then water, and dried and mounted with Permount. Images of the retina were captured at 350, 800, 1250, 1700, and 2150 µm from the optic nerve head on both the nasal and temporal sides with a 40 × objective (Leica DM6000 microscope). Images of plastic retinal sections were quantified using MetaMorph version 7.6.3 (Molecular Devices, Sunnyvale, CA, USA) and ImageJ software. Using MetaMorph, inverted red images of the Lee-stained retina, the sections were converted to monochrome to highlight cell nuclei. ImageJ was used to recognize and quantify cell nuclei as low intensity regions of interest in GCL, INL, and ONL. Average layer thicknesses were calculated by measuring the area of each layer as a smoothed polygon and dividing by the average length of the polygonal sides defining the top and bottom of each area.

Statistics

Significances of differences between multiple groups (*$P \leq 0.05$, **$P \leq 0.01$, ***$P \leq 0.001$, and ****$P \leq 0.0001$) were determined using ANOVA with Sidak correction for multiple comparisons.

Results

Ischemia Reperfusion Induces Outer Retinal Loss in Diabetic Mice

Our previous studies in the mouse IOP-induced IR injury model documented the progressive thinning of the inner retina with minimal or no outer retinal thinning.[37] We wondered if diabetes would alter the response to retinal IR injury in mice and reveal a diabetes-induced susceptibility to ischemic injury. The db/db leptin receptor deficient mouse on the C57BLKS/J (BKS) mouse background (referred to here as simply db/db) is an often-used model for type 2 diabetes mellitus (T2DM)-induced diabetic complications.[42] Homozygous db/db mice become obese at 3 to 4 weeks and hyperglycemic at 4 to 8 weeks of age (see https://www.jax.org/strain/000642). BKS db/db mice exhibit progressive inner retinal thinning from 1.5 to 9 months of age, with no significant outer retinal layer loss.[7] In this study, db/db diabetic mice and nondiabetic db/+ heterozygote controls were subjected to IR injury at 10 weeks of age, which corresponds to 2 to 6 weeks of diabetes. OCT analysis (Figs. 1A–D) was used to evaluate total inner and outer retinal thickness at 10 days following IR injury (n = 5–8 retinas/group). A significant 31% ($P < 0.0001$) loss of total retinal thickness was observed in IR injured db/db eyes (see Fig. 1B). This loss was almost entirely due to outer retinal thinning (49%, $P < 0.0001$) that only occurred in the db/db mice after IR injury (see Fig. 1D). Inner retinal layers in both db/db and db/+ eyes subjected to IR injury were on average thinner than their sham-treated counterparts, but differences did not reach significance. OCT analysis was hampered in some IR-injured eyes due to cataract formation. Therefore, eyes were harvested at 14 days following IR injury and plastic-embedded thin retinal sections were used to evaluate retinal layer thicknesses, photoreceptor nuclei densities in the ONL, and inner segment (IS) heights (Figs. 1E–J). Spider graphs showing thicknesses as a function of nasal and temporal distances from the optic nerve confirmed significant total retina thinning only in db/db eyes subjected to IR (see Fig. 1F), which was driven by loss of the outer retina (see Fig. 1H). Inner retinal thinning was evident in all groups compared to the db/+ sham group but was only significant for the db/db IR group at the innermost regions (see Fig. 1G). Nuclei counts in the ONL (see Fig. 1I) showed virtually identical results as outer retinal thickness observed by OCT, confirming photoreceptor loss. Counts of nuclei in the GCL and INL showed mostly nonsignificant trends, but it was noted that the db/+ IR group showed consistently less nuclei in the GCL than other groups (Supplementary Fig. S1). IR injury significantly reduced photoreceptor IS length ($P < 0.0001$) by 40% to 50% in the central and medial retina of db/db eyes, whereas IR had no effect on IS length in eyes of db/+ mice (see Fig. 1J). These results demonstrate that PR are normally insensitive to IR injury but are made highly susceptible to IR injury by a relatively short duration of diabetic conditions in this T2DM model.

The effect of diabetes on retinal layer thinning after IR injury was next tested in the STZ-induced type 1 diabetes mellitus (T1DM) mouse model. After 4 weeks of STZ-induced diabetes, the mice were subjected to retinal IR injury. OCT imaging (Fig. 2A) was used to evaluate total, inner and outer retinal thicknesses (Figs. 2B–D) before IR injury and over a 30-day time course after IR injury (n = 8–12 retinas/group). In nondiabetic (control) mice, IR injury caused progressive inner retinal thinning (35% by 14 days, $P < 0.0001$; see Fig. 2C), but no significant thinning of the outer retina was observed (see Fig. 2D). These results are very similar to what we previously observed in C57BL6/J mice.[37] In contrast, in STZ diabetic mice, IR induced progressive thinning of the total retina driven by outer retinal loss, such that the outer retina of STZ-IR eyes was significantly ($P < 0.0001$) thinner than all other groups, including control-IR, by 4 days after injury (see Fig. 2B). Control-IR and STZ-IR groups exhibited similar significant inner retina thinning of approximately 20% by 14 days after injury (see Fig. 2C). In contrast, IR injury caused outer retina thinning only in the STZ-IR group (see Fig. 2D), which reached a 55% decrease by 14 days ($P < 0.0001$).

To determine whether phototransduction impacted the outer retinal loss, the experiment was repeated with a set of 4-week STZ-diabetic mice with the animals separated into 2 groups and housed under normal light-cycling and continual dark conditions after IR injury (Supplementary Fig. S2). OCT analysis revealed that darkness did not prevent the thinning of the outer retina after IR injury of diabetic mice (see Supplementary Fig. S2D).

We also explored whether the duration of diabetes altered outer retinal loss after IR. Control and diabetic mice were subjected to retinal IR injury after 3 months of STZ-induced diabetes. OCT analysis was used to evaluate total, inner, and outer retinal thickness values at 10 days following IR injury (Fig. 3, n = 5–8 retinas/group). Significant outer retinal thinning occurred in the IR-injured eyes of 3-month

Investigative Ophthalmology & Visual Science

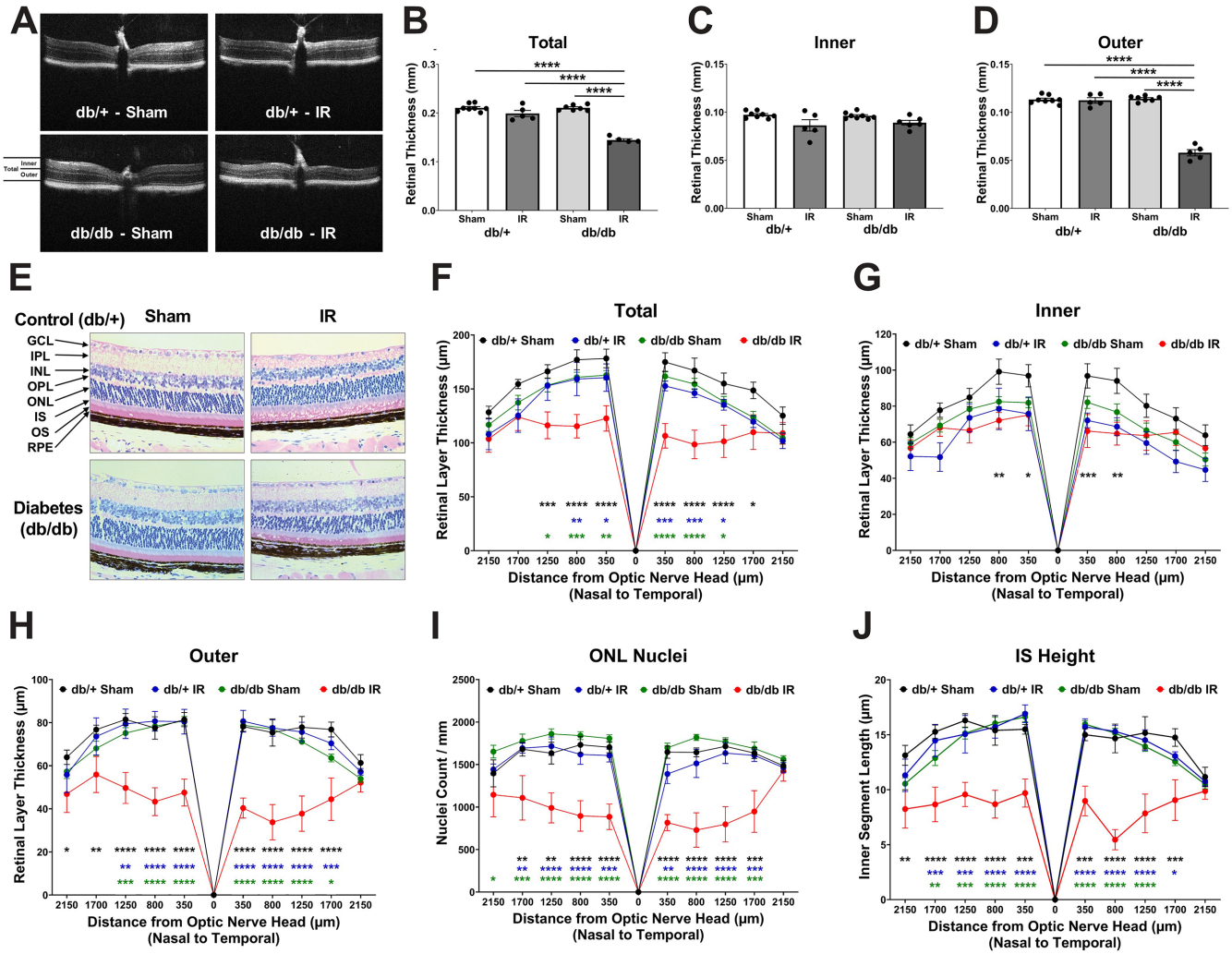

Figure 1. Retinal layer thinning after IR injury in type 2 diabetic mice. At 10 weeks of age (2–6 weeks of diabetes), db/+ (control), and db/db (diabetic) mice were subjected to retinal IR injury. OCT (**A**) was used to evaluate total (**B**), inner (**C**), and outer (D) retinal thickness at 10 days following IR injury (n = 5–8/group). At 14 days following IR injury, retinas were plastic-embedded, sectioned, and stained with Lee's stain (**E**) to evaluate total (**F**), inner (**G**), and outer (**H**) retinal thickness. The linear density of nuclei in the ONL (**I**) and the length of IS (**J**) were also evaluated. Significances of differences between groups: *$P \leq 0.05$, **$P \leq 0.01$, ***$P \leq 0.001$, and ****$P \leq 0.0001$, with colors indicating the comparison of db/db IR with each of the other groups.

diabetic mice (see Fig. 3D), which was similar to that observed in 4-week diabetic mice at 10 days after IR injury. As before, plastic sections were obtained for eyes of the 3-month diabetic cohort at 14 days following IR injury (see Fig. 3E). These were used to evaluated nuclei density in ONL (see Fig. 3F) and the length of the photoreceptor IS (see Fig. 3G). As with 1 month of diabetes, significant loss of PR nuclei ($P < 0.0001$) occurred only in diabetic mice after IR injury. However, IS length differences were not consistently reduced across the entire retina (see Fig. 3G).

Collectively, the data demonstrate that IR applied to both type 1 and type 2 mouse models of diabetes produced dramatic photoreceptor degeneration, with loss of approximately half of the outer retinal thickness within 10 to 14 days. This phenomenon is not affected by post-IR dark housing and is observed in mice after both 1 and 3 months of diabetes. The data reveal a previously unrecognized dramatic outer retinal degeneration in diabetic animals subject to transient ischemia.

IR Induces Apoptosis in STZ Diabetic Mice

Our previous study[37] used a DNA-fragmentation death assay and TUNEL to investigate retinal cell death after IR injury and found that cell death was maximal at 1 to 2 days after injury, when TUNEL-positive cells corresponded mainly to RGC and dAC in the GCL.[37] However, even though inner retinal thinning was complete by 2 weeks, a low but significantly elevated level of DNA fragmentation persisted until 3 weeks after injury, at which time TUNEL-positive cells were mainly in the ONL. To further examine how diabetes affected specific cell death we compared the distribution of TUNEL-positive cells caused by IR injury in 4-week STZ diabetic and control mice. At 1 and 4 days after IR, the retinas (n = 5/group) were harvested, and retinal frozen sections were TUNEL stained (Fig. 4). This revealed a dramatic increase in the number of TUNEL$^+$ cells in the ONL of IR-injured retina of diabetic mice at 1 day, which was significantly ($P <$ 0.0001) 4.3-fold higher than in control IR retinas (see Figs. 4A, 4B). Although appreciable numbers of TUNEL$^+$ cells

Investigative Ophthalmology & Visual Science

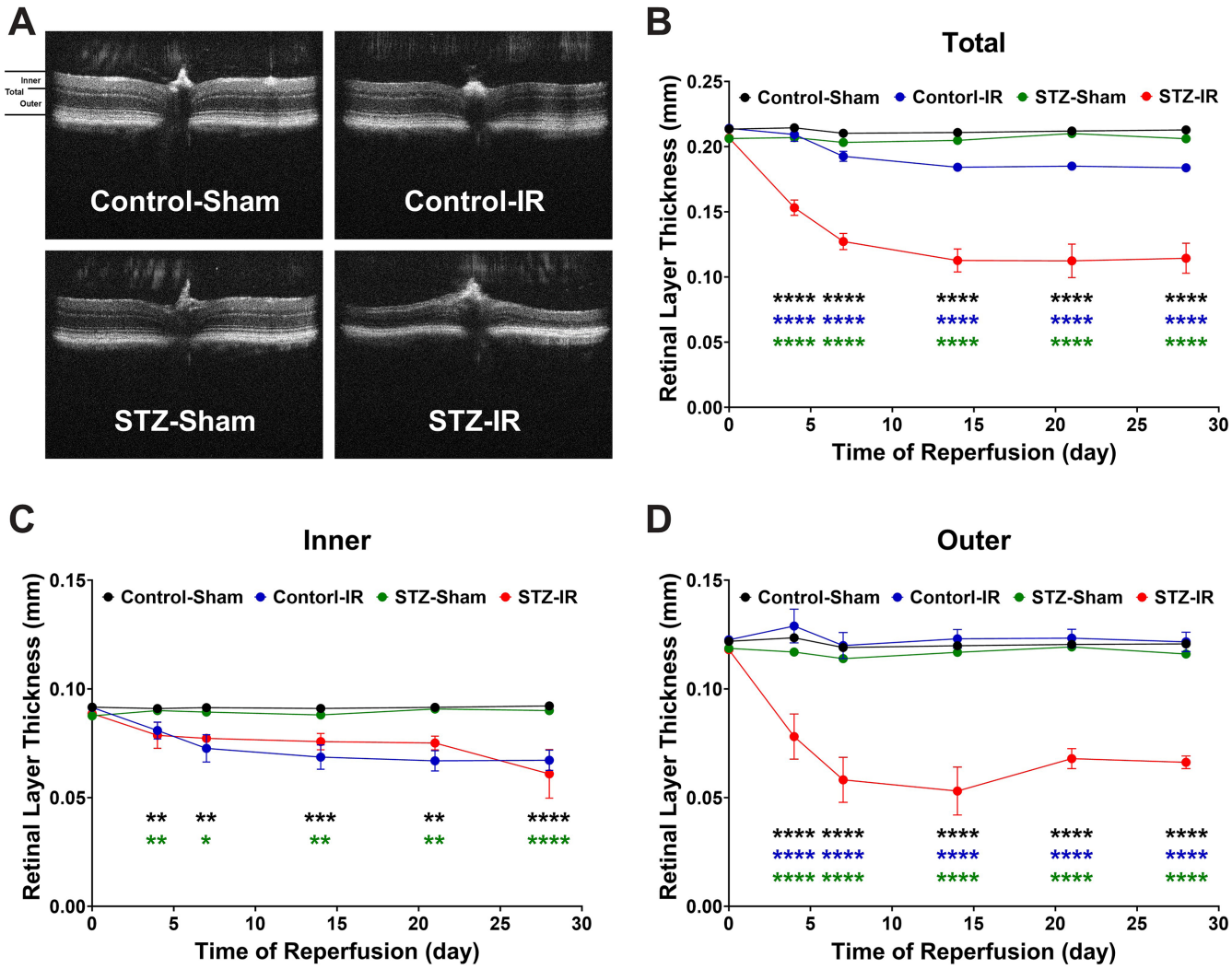

Figure 2. Time course of retinal layer thinning after IR injury in STZ-induced diabetic mice. After 4 weeks of STZ-induced diabetes, the mice were subjected to retinal IR injury. OCT (**A**) was used to evaluate total (**B**), inner (**C**), and outer (**D**) retinal thickness before IR injury and at the indicated times after IR injury (n = 8–12/group). Significances of differences between groups: *$P \leq 0.05$, **$P \leq 0.01$, ***$P \leq 0.001$, and ****$P \leq 0.0001$, with colors indicating the comparison of STZ-IR group with each other group.

were observed in other retinal layers, the increase was only significant in the ONL of IR-injured diabetic mice. At 4 days after IR injury the number of TUNEL$^+$ cells in the ONL of STZ-IR retinas had decreased from 400 cells/section to 120 cells/section and was no longer significantly higher than in the control-IR ONL (see Fig. 4C). The results confirm that diabetes induced high PR cell death after IR, with peak PR cell death at 1 day after IR injury.

The experiment was repeated and TUNEL staining was performed in whole-mounted retinas, along with IB4 staining of the vessels and Iba-1 immunofluorescence to identify microglia and invading phagocytes. The deep capillary plexus was used to identify the top of the OPL and Hoechst staining (not shown) was used to identify the ONL. Whole-mounted retinas at 2 weeks after IR injury demonstrated a significant increase in TUNEL staining in the ONL (Figs. 5A, 5B and additional images in Supplementary Fig. S3), which persisted but was reduced at 4 weeks after IR (Fig. 5C). Cell death assays were also performed for retinas harvested at 2 and 4 weeks after IR (Fig. 5D). Significant increases in DNA-fragmentation were observed in the IR injured retinas, with a significant difference between the control and diabetic retinas at 2 weeks and equivalence at 4 weeks after IR injury. Thus, this analysis confirmed that the early death response in PR is unique to IR injury of retinas under diabetic conditions and established its time course.

Vascular Permeability After IR in Diabetic Animals

We next explored the effect of diabetes on the retinal vascular response to IR injury. Previously, we demonstrated a rapid retinal vascular permeability response to IR injury, which was spontaneously resolved between 3 and 4 weeks after injury.[37] We speculated that the increased cell death observed after IR injury in diabetic mice could delay restoration of the iBRB, thus prolonging leakage. Therefore, IR injury was produced in control and 4-week STZ-diabetic mice and vascular permeability was assessed by FITC-BSA accumulation in retinal tissue after 2 and 4 weeks of recovery (Fig. 6A). In control mice, significant increases in permeabil-

Investigative Ophthalmology & Visual Science

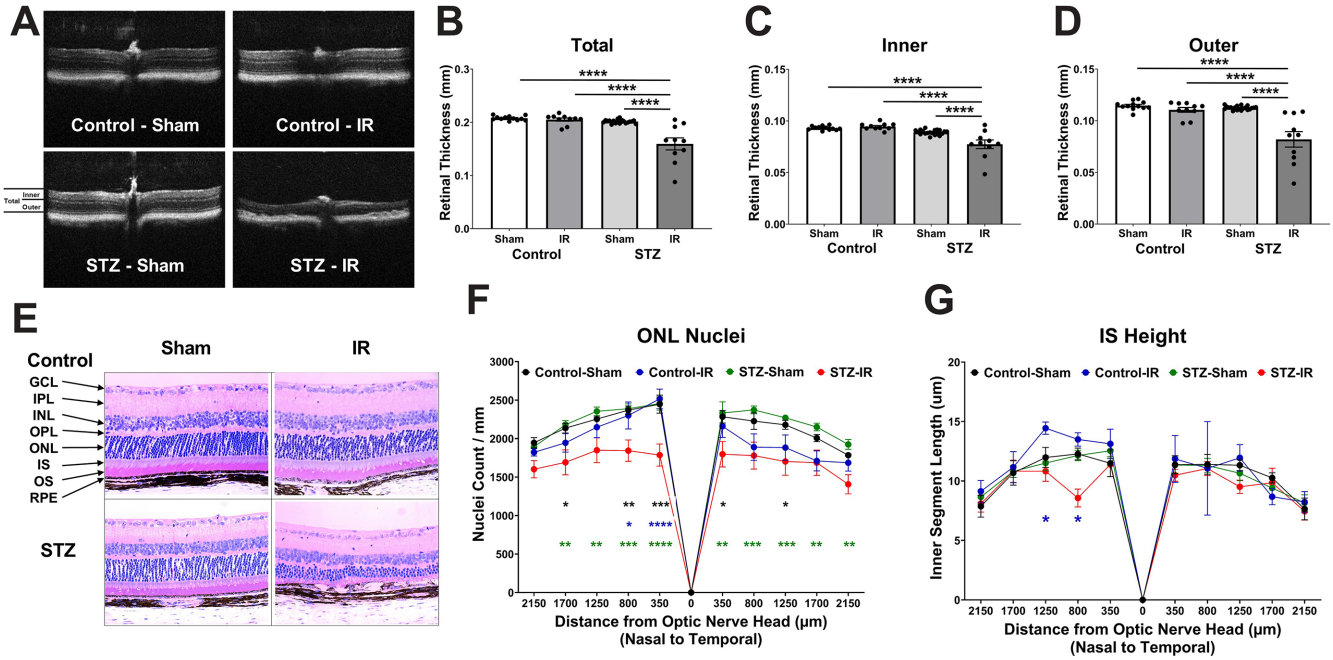

Figure 3. Retinal layer thinning after IR injury in STZ-induced diabetic mice with longer duration of diabetes. After 3 months of STZ-induced diabetes, the mice were subjected to retinal IR injury. OCT (**A**) was used to evaluate total (**B**), inner (**C**), and outer (**D**) retinal thickness at 10 days following IR injury (n = 5–8/group). At 14 days following IR injury, retinas were plastic-embedded, sectioned, and stained with Lee's stain (**E**) to evaluate the linear density of nuclei in the ONL (**F**) and the length of IS (**G**). Significances of differences between groups: *$P \leq 0.05$, **$P \leq 0.01$, ***$P \leq 0.001$, and ****$P \leq 0.0001$, with color indicating the comparison of STZ-IR with each of the other groups.

ity were observed in the IR-injured group compared to the sham group at 2 days after injury, but by 2 weeks there was no significant difference. In contrast, in diabetic mice, IR-increased permeability persisted through 4 weeks. Further, we used crosslinking and imaging of sulfo-NHS biotin to identify regions of vascular leak in flat-mounted retinas harvested 4 weeks after IR injury of control and 4 week diabetic mice (Fig. 6B). Sulfo-NHS biotin accumulation was highest at the optic nerve head and the peripheral retina, particularly in the IR-injured STZ-diabetic group. Quantification of total retinal NHS-biotin intensity per area revealed significantly increased leakage only in the STZ-diabetic IR retinas (Fig. 6C), similar to FITC-BSA accumulation. Confocal images of deep capillary plexus (Fig. 6D) revealed examples of leaking vessels in the central, peripheral, and edge of the distal retina. In contrast, there was limited NHS-biotin leak at 4 weeks after IR in nondiabetic control animals (Supplementary Fig. S4). Collectively, these studies revealed that whereas IR induced a dramatic increase in vascular permeability, the iBRB reformed within 2 to 4 weeks in the absence of diabetes. However, in diabetic animals, IR-induced permeability persisted for at least 4 weeks.

SGLT1/2 Inhibition Prevents Outer Retinal Thinning After IR in Diabetic Animals

Finally, we tested the ability of the SGLT1/2 inhibitor phlorizin to prevent outer retinal degeneration after IR in diabetic animals. Phlorizin was chosen for use because it has a long record of application in rodent diabetes models, and because phlorizin is relatively nonselective, with a half-maximal inhibitory concentration (IC_{50}) toward SGLT1 of 400 nM and an IC_{50} of 65 nM toward SGLT2.[43,44] As before, the mice were made diabetic with STZ and 4 weeks later they were subjected to IR injury. However, a group of mice were treated with phlorizin at 16 hours and 1.5 hours before the IR procedure, and treated mice were compared to vehicle injected controls. A relatively high dosage of 400 mg/kg body weight was chosen because it was previously shown to be effective at lowering blood glucose levels in T2DM mice and was also shown to directly block leptin stimulated cardiac glucose uptake in normal healthy mice.[45–47] Blood glucose measures revealed this limited phlorizin treatment reduced diabetic blood glucose compared to untreated animals but did not normalize glucose to control levels (Supplementary Fig. S5). OCT analysis (Fig. 7A) was then used to evaluate total (Fig. 7B), inner (Fig. 7C), and outer (Fig. 7D) retinal thicknesses (n = 8 retinas/group) at 10 days following IR injury. Dramatic outer retina thinning was observed in the vehicle treated IR-injured retinas, as shown above. Remarkably, retinal thinning was completely abrogated in the phlorizin-treated IR group, with outer retinal layer thinning reduced from 49% to 3% ($P < 0.0001$). At 14 days following IR injury, the eyes were harvested and plastic-embedded retina sections were obtained (n = 5–7 retinas/group; Fig. 7E). Evaluation of retinal layers confirmed that phlorizin pretreatment blocked thinning of total (Fig. 7F) and outer (Fig. 7H) retina layers. The density of nuclei in the ONL and the length of IS were also evaluated in the sections, demonstrating that loss of PR (Fig. 7I) and shortening of IS (Fig. 7J) were also abrogated by phlorizin. Collectively, these data reveal that treatment with an SGLT1/2 inhibitor, coinciding with limited blood glucose normalization, was able to completely prevent the IR-induced outer retinal loss in diabetic animals.

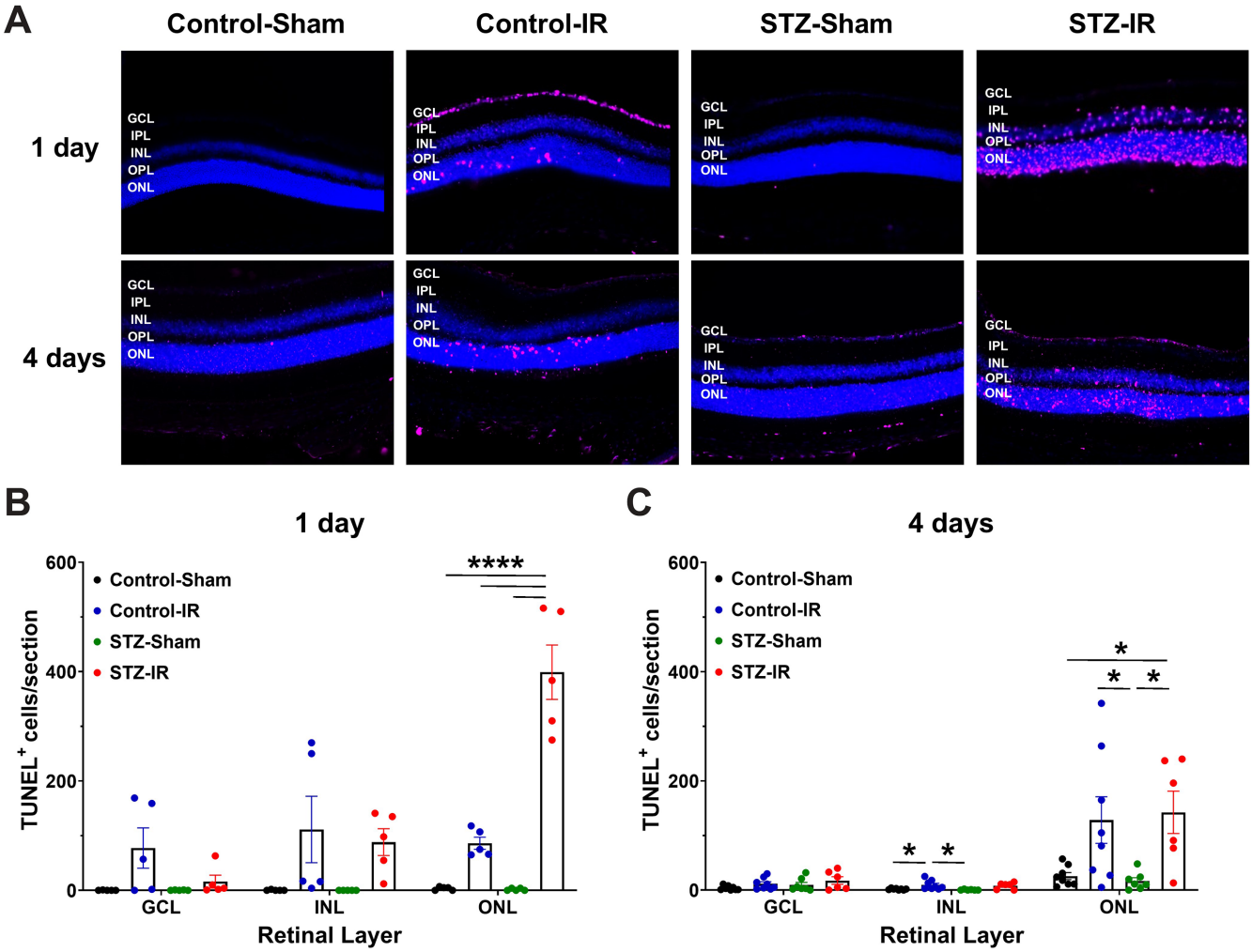

Figure 4. TUNEL staining in retinal sections in STZ-induced diabetic mice after IR injury. After 4 weeks of STZ-induced diabetes, the mice were subjected to retinal IR injury. At 1 and 4 days after injury, the retinas ($n = 5$/group) were harvested, embedded, thin sectioned, and TUNEL stained (**A**). TUNEL positive cells in different retinal layers were quantified at 1 day (**B**) and 4 days (**C**) after IR injury. Significances of differences between groups: *$P \leq 0.05$, **$P \leq 0.01$, ***$P \leq 0.001$, and ****$P \leq 0.0001$.

Discussion

In the present study, we show that both type 1 and type 2 diabetic mice exhibit dramatic outer retinal layer thinning and loss of PR following IR injury. The effect is synergistic, as IR or diabetes alone fail to induce significant PR death. The diabetic mice also demonstrated sustained vascular permeability after IR injury, potentially a result of the increased PR death. Normally, PR are relatively resistant to death following IR injury.[36] For example, our previous study in C57BL/6J mouse with the IR model of the same duration (90 minutes) of IOP-induced ischemia, showed an approximately 36% loss in inner retinal layer thickness and only a 5% loss in outer retinal layer thickness.[37] Similar inner retinal thinning with no outer retinal thinning have been observed in the rat IOP-induced retinal IR injury model.[48,49] Because of the preferential loss of RGC, the retinal IR-injury model is also referred to as "acute glaucoma."[50] However, it is well known that PR are adversely affected by IR injury. For example, electroretinogram (ERG) responses have long been used to evaluate retinal damage caused by IR and several studies show rapid and sustained decreases of both a- and b-wave amplitudes after IR injury.[51–53] This suggests that IR injury causes PR and bipolar cell dysfunction or loss, but the lack of b-wave could also be caused by loss of synaptic signaling between PR and bipolar cells.[52,54] Effects on the a-wave response could be due to inhibition of phototransduction. For example, expression levels of opsins are downregulated in mice and rats following IR injury.[51,55] In addition, several IR studies in rats have documented greater outer retinal thinning and PR loss than observed in our mouse model (for an example, see Ref. 55).

We also observed extended retinal vascular permeability in the IR and diabetes model. Previous studies revealed IR leads to a VEGF-driven increase in vascular permeability.[38–40] However, this increase in permeability resolves by 2 to 3 weeks, with retinal barrier restoration as inflammation recedes.[37] Here, we observed that permeability persisted for at least 4 weeks in the diabetic IR model. One potential mechanism by which vascular leakage may be extended is the increased release of all-trans-retinaldehyde from additional dying PR in the IR-injured retina of diabetic mice. We previously demonstrated the Lrat$^{-/-}$ genetic model, therapeutic intervention of the retinal cycle, or dark adaption

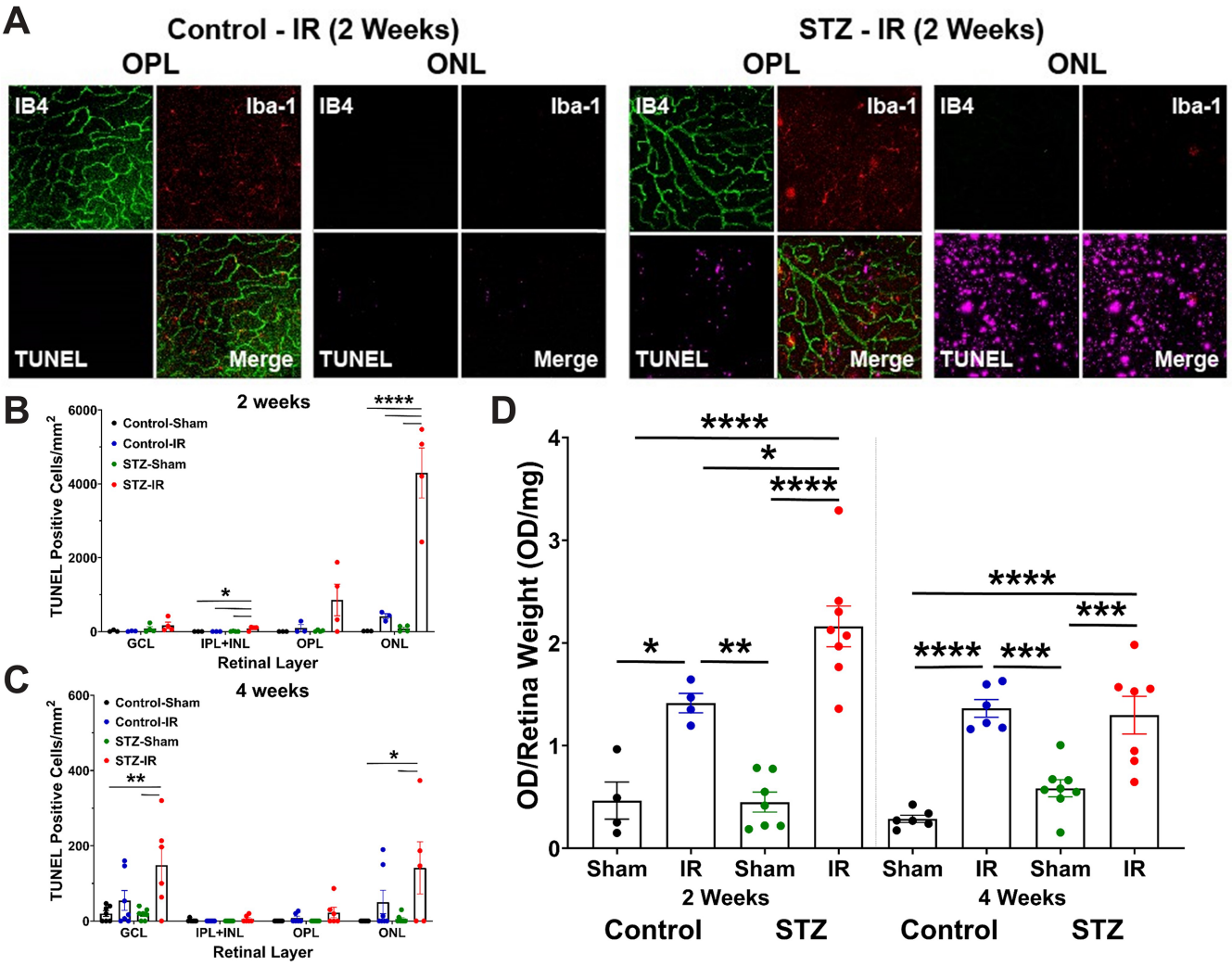

Figure 5. TUNEL staining in flat-mount retinas in STZ-induced diabetic mice after IR injury. After 4 weeks of STZ-induced diabetes, mice were subjected to retinal IR injury. At 2 and 4 weeks after injury, the retinas ($n = 5$/group) were harvested, flat-mounted, and stained for TUNEL, IB4 (vascular), and Iba-1 (microglia and invading phagocytes). Representative images from OPL and ONL at 2 weeks after IR injury are shown (**A**). TUNEL positive cells in different retinal layers were quantified at 2 weeks (**B**) and 4 weeks (**C**) after IR injury. Retinal cell death assays were performed at 2 and 4 weeks after IR injury (**D**), with optical density of the DNA fragmentation ELISA normalized to mg of retina wet weight in each reaction. Significances of differences between groups: *$P \leq 0.05$, **$P \leq 0.01$, ***$P \leq 0.001$, and ****$P \leq 0.0001$.

to reduce all-trans-retinaldehyde level each attenuated IR-induced permeability 48 hours after ischemia by approximately 50%.[56] Extended all-trans-retinaldehyde release and its potential role in extended retinal permeability after IR injury in diabetic mice remains to be tested.

The present model combining diabetes with IR-injury suggests that some aspect of diabetes causes PR to become much more sensitive to IR injury, and reversal of this sensitivity by an SGLT inhibitor suggest that hyperglycemia may be causal. The extent of hyperglycemia is a well-recognized risk factor for DR risk and progression,[57] and elevated retinal glucose is often cited as the causal factor in DR pathology.[58] Yokomizo and coworkers recently found that patients with long term diabetes but no DR, called Gold Medalists, had elevated retinol binding protein 3 (RBP3).[59] These authors also found downregulation of RBP3 expression in diabetic rodent retinas, and revealed that a protective mechanism of RBP3 is inhibition of glucose transport into the retina via glucose transporter-1 (GLUT1) binding. GLUT1-mediated glucose entry into the neural retina was also found to be necessary for retinal pathologies in the diabetic mouse.[60–63]

Mitochondrial ROS formation during reperfusion is a key mechanism of IR-induced death.[64] In addition, Du and coworkers showed that PR are the major source of reactive oxygen species in the diabetic mouse retina, and that ablation of PR inhibited the increase in retinal superoxide formation induced by diabetes.[15] Thus, a potential explanation of our results is that an increased influx of glucose during reperfusion increases ROS formation in PR such that they cannot survive the enhanced oxidative damage. However, this mechanism does not appear to account for the increased PR sensitivity in our model for several reasons. First, ketamine and xylazine anesthesia caused an increase in blood glucose,[65] such that at the time of reperfusion blood glucose levels in normal and diabetic mice were not significantly different (see Supplementary Fig. S5). Second, by immunofluorescence (IF) in retinal sections, Madrakhimov

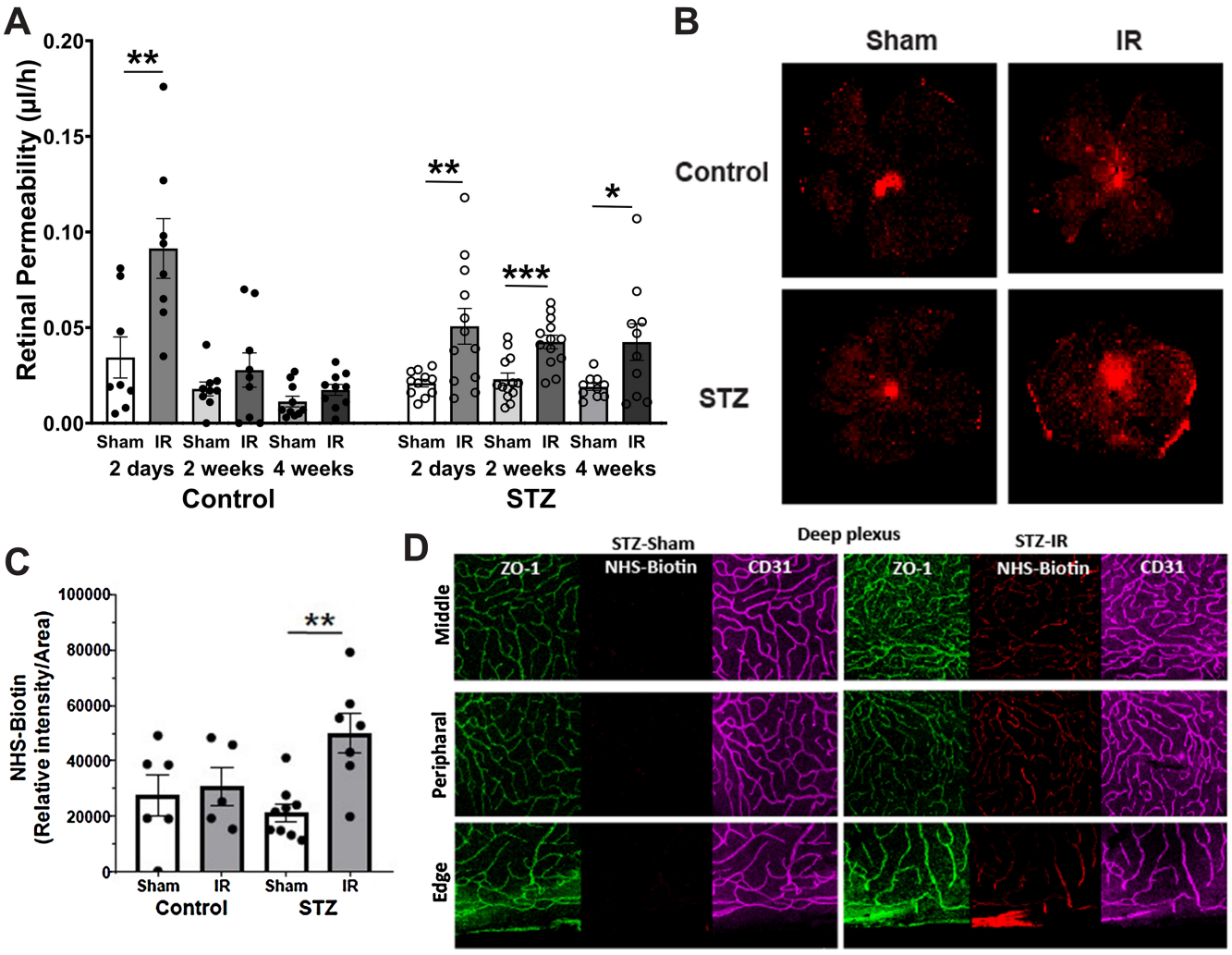

Figure 6. Effect of IR injury on retinal permeability in STZ-induced diabetic mice. At 4 weeks after STZ-induced diabetes, mice were subjected to IR injury. At the indicated times following IR injury, the retinal permeability was assessed with FITC-BSA (**A**). At 4 weeks after STZ-induced diabetes, the mice were subjected to IR injury. At 4 weeks following IR injury, the extravascular accumulation of sulfo-NHS-biotin was imaged to visualize vascular leakage (**B**). Intensity of NHS-biotin in the flat-mount retinas were quantified (**C**). Confocal images show NHS-biotin in the deep plexus (**D**). Significances of differences between groups: $^{*}P \leq 0.05$, $^{**}P \leq 0.01$, and $^{***}P \leq 0.001$.

and coworkers[61] clearly showed increased GLUT1 protein after 4 weeks of diabetes localized to the inner retina and to Müller cells, not to PR. Furthermore, Holoman and colleagues[66] showed that conditional knockout of *Glut1* in the RPE, which is expected to reduce the glucose supply to PR, did not alleviate retinal pathologies in diabetic mice. Importantly, we performed IF in retinal sections using the same antibody as used in previous studies[60–63] (Millipore #07-1401) and did not observe an increase in GLUT1 at 4 weeks of diabetes (data not shown). In addition, Madrakhimov and coworkers[61] found that GLUT1 protein expression was no longer increased after 3 months of diabetes. Such a normalization would be predicted to reverse the PR sensitivity to IR injury, but we found that the PR sensitivity was retained in 3-month diabetic mice. Finally, as a measure of oxidative damage following IR injury, we measured the accumulation of malondialdehyde (MDA), a lipid peroxidation product that is often used to quantitate oxidative damage in retinal IR injury models,[67–71] and found no difference between control-IR and diabetic IR-injured retinas (data not shown).

Pretreatment with phlorizin blocked the synergistic effects of diabetes and retinal IR injury. The current study does not provide mechanistic insight into how SGLT inhibition acts to prevent diabetes/IR outer retinal loss. However, simply reducing blood glucose levels does not seem to be the explanation because blood glucose levels at the time of IR injury were not normalized by the treatment. It is possible that phlorizin has direct effects on PR in the diabetic retina. Intriguingly, a recent study showed that intravitreal injection of the SGLT2 inhibitor (SGLT2i) empagliflozin largely prevented inner retinal thinning and inflammation after IOP-induced IR injury in normal healthy mice.[72] The protective and anti-inflammatory effects of empagliflozin were attributed to its ability to promote mitochondrial fusion and prevent ROS production in RGC. We observed that systemic phlorizin treatment reduced inner retinal layer thinning after IR injury, but the effects were not significant (see Fig. 7C) and not consistent between nasal and temporal retina (see Fig. 7G).

Phlorizin is a natural sodium-glucose co-transporter inhibitor that led to development of the synthetic sodium-

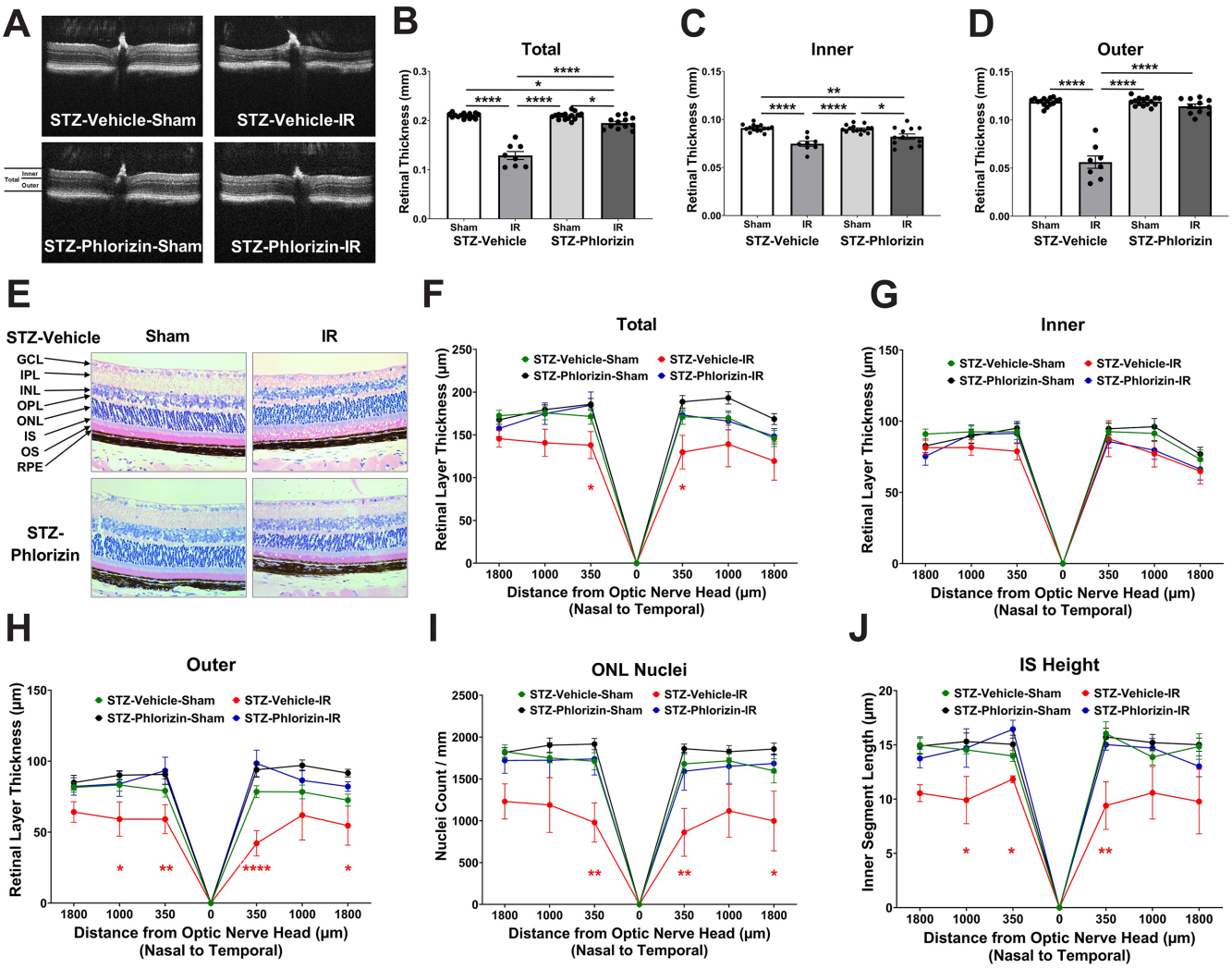

Figure 7. Effect of a SGLT1/2 inhibitor on retinal layer thinning. After 4 weeks of STZ-induced diabetes, the mice were treated twice (16 and 1.5 hours before ischemia) with an SGLT inhibitor (phlorizin, 400 mg/kg, intraperitoneally [IP]) or carrier prior to retinal IR injury. OCT (**A**) was used to evaluate total (**B**), inner (**C**), and outer (**D**) retinal thickness at 10 days following IR injury ($n = 8$/group). At 14 days following IR injury, retinas were plastic-embedded, sectioned and stained with Lee's stain (**E**) to evaluate total (**F**), inner (**G**), and outer (**H**) retinal thickness. The linear density of nuclei in the ONL (**I**) and the length of IS (**J**) were also evaluated. Significances of differences between groups: *$P \leq 0.05$, **$P \leq 0.01$, ***$P \leq 0.001$, and ****$P \leq 0.0001$, with red color in **F** to **J** indicating the comparison between the STZ-vehicle-IR and the STZ-phlorizin-IR groups.

glucose co-transporter 2 inhibitor class of drugs now widely prescribed for patients with diabetes. Phlorizin exhibits an approximate 6-fold selectivity for SGLT2 over SGLT1, which is much lower than most SGLT2is used clinically.[43] Blocking SGLT2 reduces hyperglycemia by inhibiting glucose reuptake in the kidneys. Additional inhibition of SGLT1 with high doses of phlorizin has the advantage of also blocking SGLT1-mediated glucose uptake in the kidney and intestine.[43] Less selective SGLT2is exhibit clinical benefits in patients with diabetes, particularly preventing heart failure and renal disease.[73] SGLT2is with relatively low selectivity for SGLT2 over SGLT1 (SGLTis) also lower the risk of stroke in patients with type 2 diabetes.[74] Notably, the ability of relatively nonselective SGLTis to protect against diabetic complications is not explained by reduction of hyperglycemia because other anti-diabetic treatments with larger effects on blood glucose and HbA1c levels do not cause the same protective effects as SGLTis, and SGLTis exhibit protective effects against heart failure in non-diabetic patients.[75] Rather, it is thought that SGLTis exert direct protective effects on tissues, and a multitude of potential mechanisms have been examined, especially in cardiomyocytes, which express SGLT1.[76,77] Further studies are needed to determine if phlorizin or other SGLTis can directly protect PR in diabetic retinas from IR injury.

Studies have examined the effects of SGLTis in experimental diabetic retinopathy models. Fort and coworkers[78] revealed that phlorizin treatment for 4 days nearly abrogated retinal cell death and reversed Müller cell gliosis. Protection coincided with normalization of retinal glucose content, and with increased insulin receptor kinase and Akt activities in the retina. Hi and colleagues[79] showed that dapagliflozin treatment of STZ-diabetic mice for 12 weeks largely prevented retinal thinning. The neuroprotective effect was not duplicated by insulin treatment for the same period, even though insulin lowered blood glucose and HbA1c levels to the same extents as dapagliflozin.

Madrakhimov et al.[61] found that 10 days of treatment of STZ-diabetic mice with phlorizin prevented death and lowered cleaved caspase-3 in RGC, which was attributed to activation of autophagy downstream of mechanistic target of rapamycin (mTOR) complex 1. Eid and colleagues[80] showed reductions in DRN after 10 weeks of treatment of STZ-diabetic and db/db mice with empagliflozin. Recently, Yamamoto and coworkers[81] employed a mouse model using a single very high dose of STZ (150 kg/mg) to examine the effects of SGLTis on retinal pathologies. This model exhibits rapid retinal inflammation and edema after STZ treatment. The authors showed that treatment of this model with ipragliflozin or luseogliflozin blocked signs of microglial activation at 2 weeks after STZ, lowered expression of VEGF-A, VEGF receptor, and Ang2 at 4 weeks after STZ, and blocked capillary dropout at 4 weeks after STZ treatment. Remarkably, low doses of the SGLTis were as effective as high doses, even though blood glucose levels in all four treatment groups were in the diabetic range and the glucose levels in the two low dosage SGLTi treatment groups were not significantly different than the untreated STZ group. It should be noted that the multiple low dose STZ mouse model used in the present study does not exhibit overt signs of retinal pathology at 2 or 4 weeks of diabetes, and does not exhibit retinal edema or develop significant capillary dropout until after 6 to 9 months of diabetes.[82]

Recently, several large retrospective clinical studies and META analyses have examined potential benefits of SGLT2is for lowering DR risk and progression. These studies have either found no increased risk[83–85] or significantly decreased risk[84,86–90] of DR onset associated with SGLT2i use. Li and coworkers found that SGLT2i use initially increased the risk of DR, whereas longer-term (>2 years) use considerably lowered risk of DR.[91] A META analysis by Ma and colleagues[92] found that SGLT2i use lowered DR risk only in patients with less than 10 years duration of diabetes. In contrast, Lin et al.[93] found that the risk of DR onset was not affected, but the risk of progression to PDR was considerably lowered with SGLT2i use. Ishibashi and coworkers performed an insurance claims database analysis including 11 million Japanese patients revealing that SGLT2i use reduced the frequency of anti-VEGF treatments required to treat DME.[94] In this way, SGLT2i treatment may represent an adjuvant treatment for DME. Furthermore, a topical eye drop formulation containing the SGLT2i enavogliflozin (Daewoong Therapeutics Inc., DWRX2008) is under development as a primary treatment for DR and DME.[95]

In conclusion, the current study revealed that retinal IR injury applied to rodent models of diabetes induced a dramatic and rapid loss of PR that was not observed in nondiabetic control IR animals. This was associated with a prolonged period of increased vascular permeability. Phlorizin pretreatment effectively prevented this loss of PR, with limited effects on blood glucose. The data are consistent with the development of dual SLGTis to treat diabetic complications including DR.

Acknowledgments

Supported by a National Institutes of Health (NIH) grant R01EY029349 to D.A.A. and S.F.A.; NIH grant R01EY012021 to D.A.A.; NIH grant R01EY031961 to S.F.A.; Research to Prevent Blindness grants to D.A.A. and S.F.A.; NIH P30EY007003, Michigan Vision Center Core Grant; NIH grant P30DK020572, Michigan Diabetes Research Center; and NIH instrumentation grant S10OD028612.

Disclosure: **D.A. Antonetti**, None; **C.M. Lin**, None; **S. Shanmugam**, None; **H. Hager**, None; **M. Cao**, None; **X. Liu**, None; **A. Dreffs**, None; **A. Habash**, None; **S.F. Abcouwer**, None

References

1. Antonetti DA, Silva PS, Stitt AW. Current understanding of the molecular and cellular pathology of diabetic retinopathy. *Nat Rev Endocrinol*. 2021;17:195–206.
2. Bahr TA, Bakri SJ. Update on the management of diabetic retinopathy: anti-VEGF agents for the prevention of complications and progression of nonproliferative and proliferative retinopathy. *Life (Basel)*. 2023;13:1098.
3. Agostini H, Abreu F, Baumal CR, et al. Faricimab for neovascular age-related macular degeneration and diabetic macular edema: from preclinical studies to phase 3 outcomes [published online ahead of print June 7, 2024]. *Graefes Arch Clin Exp Ophthalmol*, doi:10.1007/s00417-024-06531-9.
4. Lynch SK, Abramoff MD. Diabetic retinopathy is a neurodegenerative disorder. *Vision Res*. 2017;139:101–107.
5. Channa R, Wolf RM, Simo R, et al. A new approach to staging diabetic eye disease: staging of diabetic retinal neurodegeneration and diabetic macular edema. *Ophthalmol Sci*. 2024;4:100420.
6. Zhou J, Chen B. Retinal cell damage in diabetic retinopathy. *Cells*. 2023;12:1342.
7. Sheskey SR, Antonetti DA, Renteria RC, Lin CM. Correlation of retinal structure and visual function assessments in mouse diabetes models. *Invest Ophthalmol Vis Sci*. 2021;62:20.
8. Goncalves A, Dreffs A, Lin CM, et al. Vascular expression of permeability-resistant occludin mutant preserves visual function in diabetes. *Diabetes*. 2021;70:1549–1560.
9. McAnany JJ, Persidina OS, Park JC. Clinical electroretinography in diabetic retinopathy: a review. *Surv Ophthalmol*. 2022;67:712–722.
10. Tonade D, Kern TS. Photoreceptor cells and RPE contribute to the development of diabetic retinopathy. *Prog Retin Eye Res*. 2021;83:100919.
11. Rajagopal R, Kern T. Clinical evidence of a photoreceptor origin in diabetic retinal disease. *Ophthalmol Sci*. 2025;5:100591.
12. Sternberg P, Jr., Landers MB, 3rd, Wolbarsht M. The negative coincidence of retinitis pigmentosa and proliferative diabetic retinopathy. *Am J Ophthalmol*. 1984;97:788–789.
13. Arden GB. The absence of diabetic retinopathy in patients with retinitis pigmentosa: implications for pathophysiology and possible treatment. *Br J Ophthalmol*. 2001;85:366–370.
14. Liu H, Tang J, Du Y, et al. Transducin1, phototransduction and the development of early diabetic retinopathy. *Invest Ophthalmol Vis Sci*. 2019;60:1538–1546.
15. Du Y, Veenstra A, Palczewski K, Kern TS. Photoreceptor cells are major contributors to diabetes-induced oxidative stress and local inflammation in the retina. *Proc Natl Acad Sci USA*. 2013;110:16586–16591.
16. Liu H, Tang J, Du Y, et al. Retinylamine benefits early diabetic retinopathy in mice. *J Biol Chem*. 2015;290:21568–21579.
17. Antropoli A, Arrigo A, La Franca L, et al. Peripheral and central capillary non-perfusion in diabetic retinopathy: an updated overview. *Front Med (Lausanne)*. 2023;10:1125062.
18. Datlinger F, Wassermann L, Reumueller A, et al. Assessment of detailed photoreceptor structure and retinal sensitivity in diabetic macular ischemia using adaptive optics-OCT and microperimetry. *Invest Ophthalmol Vis Sci*. 2021;62:1.

19. Nesper PL, Scarinci F, Fawzi AA. Adaptive optics reveals photoreceptor abnormalities in diabetic macular ischemia. *PLoS One*. 2017;12:e0169926.
20. Scarinci F, Jampol LM, Linsenmeier RA, Fawzi AA. Association of diabetic macular nonperfusion with outer retinal disruption on optical coherence tomography. *JAMA Ophthalmol*. 2015;133:1036–1044.
21. Scarinci F, Nesper PL, Fawzi AA. Deep retinal capillary nonperfusion is associated with photoreceptor disruption in diabetic macular ischemia. *Am J Ophthalmol*. 2016;168:129–138.
22. Scarinci F, Varano M, Parravano M. Retinal sensitivity loss correlates with deep capillary plexus impairment in diabetic macular ischemia. *J Ophthalmol*. 2019;2019:7589841.
23. Scuderi L, Fragiotta S, Di Pippo M, Abdolrahimzadeh S. The role of diabetic choroidopathy in the pathogenesis and progression of diabetic retinopathy. *Int J Mol Sci*. 2023;24:10167.
24. Dai Y, Zhou H, Chu Z, et al. Microvascular changes in the choriocapillaris of diabetic patients without retinopathy investigated by swept-source OCT angiography. *Invest Ophthalmol Vis Sci*. 2020;61:50.
25. Endo H, Kase S, Ito Y, et al. Relationship between choroidal structure and duration of diabetes. *Graefes Arch Clin Exp Ophthalmol*. 2019;257:1133–1140.
26. Hamadneh T, Aftab S, Sherali N, Vetrivel Suresh R, Tsouklidis N, An M. Choroidal changes in diabetic patients with different stages of diabetic retinopathy. *Cureus*. 2020;12:e10871.
27. Huang X, Zhang P, Zou X, et al. Thinner average choroidal thickness is a risk factor for the onset of diabetic retinopathy. *Ophthalmic Res*. 2020;63:259–270.
28. Jiang J, Liu J, Yang J, Jiang B. Optical coherence tomography evaluation of choroidal structure changes in diabetic retinopathy patients: a systematic review and meta-analysis. *Front Med (Lausanne)*. 2022;9:986209.
29. Kase S, Endo H, Takahashi M, et al. Choroidal vascular structures in diabetic patients: a meta-analysis. *Graefes Arch Clin Exp Ophthalmol*. 2021;259:3537–3548.
30. Temel E, Özcan G, Yanık Ö, et al. Choroidal structural alterations in diabetic patients in association with disease duration, HbA1c level, and presence of retinopathy. *Int Ophthalmol*. 2022;42:3661–3672.
31. Zhang S, Zhu Z, Bulloch G, et al. Progressive peripapillary choroid thinning and retinal neurodegeneration in patients with diabetes: a 3-year cohort study. *Retina*. 2022;42:2401–2410.
32. Wang W, Li L, Wang J, et al. Macular choroidal thickness and the risk of referable diabetic retinopathy in type 2 diabetes: a 2-year longitudinal study. *Invest Ophthalmol Vis Sci*. 2022;63:9.
33. Dou N, Li G, Fang D, Zhang S, Liang X, Yu S. Association between choroidopathy and photoreceptors during the early stage of diabetic retinopathy: a cross-sectional study. *Graefes Arch Clin Exp Ophthalmol*. 2023;262:1121–1129.
34. Parravano M, Ziccardi L, Borrelli E, et al. Outer retina dysfunction and choriocapillaris impairment in type 1 diabetes. *Sci Rep*. 2021;11:15183.
35. Ro-Mase T, Ishiko S, Omae T, Ishibazawa A, Shimouchi A, Yoshida A. Association between alterations of the choriocapillaris microcirculation and visual function and cone photoreceptors in patients with diabetes. *Invest Ophthalmol Vis Sci*. 2020;61:1.
36. Osborne NN, Casson RJ, Wood JP, Chidlow G, Graham M, Melena J. Retinal ischemia: mechanisms of damage and potential therapeutic strategies. *Prog Retin Eye Res*. 2004;23:91–147.
37. Abcouwer SF, Shanmugam S, Muthusamy A, et al. Inflammatory resolution and vascular barrier restoration after retinal ischemia reperfusion injury. *J Neuroinflammation*. 2021;18:186.
38. Abcouwer SF, Lin CM, Wolpert EB, et al. Effects of ischemic preconditioning and bevacizumab on apoptosis and vascular permeability following retinal ischemia-reperfusion injury. *Invest Ophthalmol Vis Sci*. 2010;51:5920–5933.
39. Muthusamy A, Lin CM, Shanmugam S, Lindner HM, Abcouwer SF, Antonetti DA. Ischemia-reperfusion injury induces occludin phosphorylation/ubiquitination and retinal vascular permeability in a VEGFR-2-dependent manner. *J Cereb Blood Flow Metab*. 2014;34:522–531.
40. Canonica J, Foxton R, Garrido MG, et al. Delineating effects of angiopoietin-2 inhibition on vascular permeability and inflammation in models of retinal neovascularization and ischemia/reperfusion. *Front Cell Neurosci*. 2023;17:1192464.
41. Liu X, Dreffs A, Díaz-Coránguez M, et al. Occludin S490 phosphorylation regulates vascular endothelial growth factor-induced retinal neovascularization. *Am J Pathol*. 2016;186:2486–2499.
42. Sun Z, Liu Y, Zhao Y, Xu Y. Animal models of type 2 diabetes complications: a review. *Endocr Res*. 2024;49:46–58.
43. Dominguez Rieg JA, Rieg T. What does sodium-glucose cotransporter 1 inhibition add: prospects for dual inhibition. *Diabetes Obes Metab*. 2019;21(Suppl 2):43–52.
44. Rieg T, Vallon V. Development of SGLT1 and SGLT2 inhibitors. *Diabetologia*. 2018;61:2079–2086.
45. Banerjee SK, McGaffin KR, Pastor-Soler NM, Ahmad F. SGLT1 is a novel cardiac glucose transporter that is perturbed in disease states. *Cardiovasc Res*. 2009;84:111–118.
46. David-Silva A, Esteves JV, Morais M, et al. Dual SGLT1/SGLT2 inhibitor phlorizin ameliorates non-alcoholic fatty liver disease and hepatic glucose production in type 2 diabetic mice. *Diabetes Metab Syndr Obes*. 2020;13:739–751.
47. Shimo S, Saitoh S, Nguyen HB, et al. Sodium-glucose cotransporter (SGLT) inhibitor restores lost axonal varicosities of the myenteric plexus in a mouse model of high-fat diet-induced obesity. *Sci Rep*. 2020;10:12372.
48. Schmid H, Renner M, Dick HB, Joachim SC. Loss of inner retinal neurons after retinal ischemia in rats. *Invest Ophthalmol Vis Sci*. 2014;55:2777–2787.
49. Rosenbaum DM, Rosenbaum PS, Singh M, et al. Functional and morphologic comparison of two methods to produce transient retinal ischemia in the rat. *J Neuroophthalmol*. 2001;21:62–68.
50. Skowronska-Krawczyk D, Zhao L, Zhu J, et al. P16INK4a upregulation mediated by SIX6 defines retinal ganglion cell pathogenesis in glaucoma. *Mol Cell*. 2015;59:931–940.
51. Wiemann S, Yousf A, Joachim SC, et al. Knock-out of tenascin-C ameliorates ischemia-induced rod-photoreceptor degeneration and retinal dysfunction. *Front Neurosci*. 2021;15:642176.
52. Sun D, Bui BV, Vingrys AJ, Kalloniatis M. Alterations in photoreceptor-bipolar cell signaling following ischemia/reperfusion in the rat retina. *J Comp Neurol*. 2007;505:131–146.
53. Zhu Y, Ohlemiller KK, McMahan BK, Gidday JM. Mouse models of retinal ischemic tolerance. *Invest Ophthalmol Vis Sci*. 2002;43:1903–1911.
54. Fu Y, Hu T, Zhang Q, et al. Transneuronal degeneration in the visual pathway of rats following acute retinal ischemia/reperfusion. *Dis Markers*. 2021;2021:2629150.
55. Palmhof M, Frank V, Rappard P, et al. From ganglion cell to photoreceptor layer: timeline of deterioration in a rat ischemia/reperfusion model. *Front Cell Neurosci*. 2019;13:174.

Investigative Ophthalmology & Visual Science

56. Dreffs A, Lin CM, Liu X, et al. All-trans-retinaldehyde contributes to retinal vascular permeability in ischemia reperfusion. *Invest Ophthalmol Vis Sci*. 2020;61:8.
57. Klein R, Lee KE, Gangnon RE, Klein BE. The 25-year incidence of visual impairment in type 1 diabetes mellitus the Wisconsin epidemiologic study of diabetic retinopathy. *Ophthalmology*. 2010;117:63–70.
58. Zhang C, Gu L, Xie H, et al. Glucose transport, transporters and metabolism in diabetic retinopathy. *Biochim Biophys Acta Mol Basis Dis*. 2024;1870:166995.
59. Yokomizo H, Maeda Y, Park K, et al. Retinol binding protein 3 is increased in the retina of patients with diabetes resistant to diabetic retinopathy. *Sci Transl Med*. 2019;11(499):eaau6627.
60. Holoman NC, Aiello JJ, Trobenter TD, et al. Reduction of Glut1 in the neural retina but not the RPE alleviates polyol accumulation and normalizes early characteristics of diabetic retinopathy. *J Neurosci*. 2021;41:3275–3299.
61. Madrakhimov SB, Yang JY, Kim JH, Han JW, Park TK. mTOR-dependent dysregulation of autophagy contributes to the retinal ganglion cell loss in streptozotocin-induced diabetic retinopathy. *Cell Commun Signal*. 2021;19:29.
62. You ZP, Zhang YL, Shi K, et al. Suppression of diabetic retinopathy with GLUT1 siRNA. *Sci Rep*. 2017;7:7437.
63. Aiello JJ, Bogart MC, Chan WT, et al. Systemic reduction of Glut1 normalizes retinal dysfunction, inflammation, and oxidative stress in the retina of spontaneous type 2 diabetic mice. *Am J Pathol*. 2023;193:927–938.
64. Chouchani ET, Pell VR, James AM, et al. A unifying mechanism for mitochondrial superoxide production during ischemia-reperfusion injury. *Cell Metab*. 2016;23:254–263.
65. Brown ET, Umino Y, Loi T, Solessio E, Barlow R. Anesthesia can cause sustained hyperglycemia in C57/BL6J mice. *Vis Neurosci*. 2005;22:615–618.
66. Holoman NC, Aiello JJ, Trobenter TD, et al. Reduction of Glut1 in the neural retina but not the RPE alleviates polyol accumulation and normalizes early characteristics of diabetic retinopathy. *J Neurosci*. 2021;41:3275–3299.
67. Ayala A, Muñoz MF, Argüelles S. Lipid peroxidation: production, metabolism, and signaling mechanisms of malondialdehyde and 4-hydroxy-2-nonenal. *Oxid Med Cell Longev*. 2014;2014:360438.
68. Yao F, Peng J, Zhang E, et al. Pathologically high intraocular pressure disturbs normal iron homeostasis and leads to retinal ganglion cell ferroptosis in glaucoma. *Cell Death Differ*. 2023;30:69–81.
69. Mei T, Wu J, Wu K, et al. Lipocalin 2 induces visual impairment by promoting ferroptosis in retinal ischemia-reperfusion injury. *Ann Transl Med*. 2023;11:3.
70. Wang J, Sun Z, Shen J, et al. Octreotide protects the mouse retina against ischemic reperfusion injury through regulation of antioxidation and activation of NF-κB. *Oxid Med Cell Longev*. 2015;2015:970156.
71. Xu YP, Han F, Tan J. Edaravone protects the retina against ischemia/reperfusion induced oxidative injury through the PI3K/Akt/Nrf2 pathway. *Mol Med Rep*. 2017;16:9210–9216.
72. Yang Z, Liu Y, Chen X, et al. Empagliflozin targets Mfn1 and Opa1 to attenuate microglia-mediated neuroinflammation in retinal ischemia and reperfusion injury. *J Neuroinflammation*. 2023;20:296.
73. Zelniker TA, Braunwald E. Clinical benefit of cardiorenal effects of sodium-glucose cotransporter 2 inhibitors: JACC State-of-the-Art Review. *J Am Coll Cardiol*. 2020;75:435–447.
74. Sayour AA, Oláh A, Ruppert M, Barta BA, Merkely B, Radovits T. Effect of pharmacological selectivity of SGLT2 inhibitors on cardiovascular outcomes in patients with type 2 diabetes: a meta-analysis. *Sci Rep*. 2024;14:2188.
75. Dyck JRB, Sossalla S, Hamdani N, et al. Cardiac mechanisms of the beneficial effects of SGLT2 inhibitors in heart failure: evidence for potential off-target effects. *J Mol Cell Cardiol*. 2022;167:17–31.
76. Huang K, Luo X, Liao B, Li G, Feng J. Insights into SGLT2 inhibitor treatment of diabetic cardiomyopathy: focus on the mechanisms. *Cardiovasc Diabetol*. 2023;22:86.
77. Sayour AA, Ruppert M, Oláh A, et al. Effects of SGLT2 inhibitors beyond glycemic control-focus on myocardial SGLT1. *Int J Mol Sci*. 2021;22:9852.
78. Fort PE, Losiewicz MK, Reiter CE, et al. Differential roles of hyperglycemia and hypoinsulinemia in diabetes induced retinal cell death: evidence for retinal insulin resistance. *PLoS One*. 2011;6:e26498.
79. Hu Y, Xu Q, Li H, et al. Dapagliflozin reduces apoptosis of diabetic retina and human retinal microvascular endothelial cells through ERK1/2/cPLA2/AA/ROS pathway independent of hypoglycemic. *Front Pharmacol*. 2022;13:827896.
80. Eid SA, O'Brien PD, Hinder LM, et al. Differential effects of empagliflozin on microvascular complications in murine models of type 1 and type 2 diabetes. *Biology (Basel)*. 2020;9:347.
81. Yamato M, Kato N, Yamada KI, Inoguchi T. The early pathogenesis of diabetic retinopathy and its attenuation by sodium-glucose transporter 2 inhibitors. *Diabetes*. 2024;73:1153–1166.
82. Feit-Leichman RA, Kinouchi R, Takeda M, et al. Vascular damage in a mouse model of diabetic retinopathy: relation to neuronal and glial changes. *Invest Ophthalmol Vis Sci*. 2005;46:4281–4287.
83. Tan L, Wang Z, Okoth K, et al. Associations of antidiabetic drugs with diabetic retinopathy in people with type 2 diabetes: an umbrella review and meta-analysis. *Front Endocrinol (Lausanne)*. 2023;14:1303238.
84. Małyszczak A, Przeździecka-Dołyk J, Szydełko-Paśko U, Misiuk-Hojło M. Novel antidiabetic drugs and the risk of diabetic retinopathy: a systematic review and meta-analysis of randomized controlled trials. *J Clin Med*. 2024;13:1797.
85. Li C, Zhou Z, Neuen BL, et al. Sodium-glucose cotransporter-2 inhibition and ocular outcomes in patients with type 2 diabetes: a systematic review and meta-analysis. *Diabetes Obes Metab*. 2021;23:252–257.
86. Yen FS, Wei JC, Yu TS, Hung YT, Hsu CC, Hwu CM. Sodium-glucose cotransporter 2 inhibitors and risk of retinopathy in patients with type 2 diabetes. *JAMA Netw Open*. 2023;6:e2348431.
87. Huang ST, Bair PJ, Chang SS, et al. Risk of diabetic retinopathy in patients with type 2 diabetes after SGLT-2 inhibitors: a nationwide population cohort study. *Clin Pharmacol Ther*. 2024;115:95–103.
88. Eleftheriadou A, Riley D, Zhao SS, et al. Risk of diabetic retinopathy and diabetic macular oedema with sodium-glucose cotransporter 2 inhibitors and glucagon-like peptide 1 receptor agonists in type 2 diabetes: a real-world data study from a global federated database. *Diabetologia*. 2024;67:1271–1282.
89. Hasselstrøm Jensen J, Vestergaard P, Hasselstrøm Jensen M. Association between glucose-lowering treatments and risk of diabetic retinopathy in people with type 2 diabetes: a nationwide cohort study. *Curr Drug Saf*. 2024;19:236–243.
90. Chung YR, Ha KH, Lee K, Kim DJ. Effects of sodium-glucose cotransporter-2 inhibitors and dipeptidyl peptidase-4 inhibitors on diabetic retinopathy and its progression: a real-world Korean study. *PLoS One*. 2019;14:e0224549.
91. Li JX, Hung YT, Bair H, Hsu SB, Hsu CY, Lin CJ. Sodium-glucose co-transporter 2 inhibitor add-on therapy for metformin delays diabetic retinopathy progression in

diabetes patients: a population-based cohort study. *Sci Rep*. 2023;13:17049.

92. Ma Y, Lin C, Cai X, et al. The association between the use of sodium glucose cotransporter 2 inhibitor and the risk of diabetic retinopathy and other eye disorders: a systematic review and meta-analysis. *Expert Rev Clin Pharmacol*. 2022;15:877–886.
93. Lin TY, Kang EY, Shao SC, et al. Risk of diabetic retinopathy between sodium-glucose cotransporter-2 inhibitors and glucagon-like peptide-1 receptor agonists. *Diabetes Metab J*. 2023;47:394–404.
94. Ishibashi R, Inaba Y, Koshizaka M, et al. Sodium-glucose cotransporter 2 inhibitor therapy reduces the administration frequency of anti-vascular endothelial growth factor agents in patients with diabetic macular oedema with a history of anti-vascular endothelial growth factor agent use: a cohort study using the Japanese health insurance claims database. *Diabetes Obes Metab*. 2024;26:1510–1518.
95. Jang M, Kang M, Lee E, Shin D. Ocular and plasma pharmacokinetics of enavogliflozin ophthalmic solution in preclinical species. *Pharmaceuticals (Basel)*. 2024;17:111.

Investigative Ophthalmology & Visual Science